The ENSO Signal in the Stratosphere

Natalia Calvo,[a,b] Ricardo García-Herrera,[b] and Rolando R. Garcia[a]

[a]*National Center for Atmospheric Research, Atmospheric Chemistry Division, Boulder, Colorado, USA*

[b]*Universidad Complutense de Madrid, Ciudad Universitaria Madrid, Madrid, Spain*

Although the El Niño–Southern Oscillation (ENSO) is a tropospheric phenomenon, its effects are also observed in the stratosphere. Traditionally, the study of ENSO above the troposphere has been difficult because of the lack of global observations at high altitudes and also because of the presence of other sources of variability whose signals are difficult to disentangle from ENSO effects. Recent work with general circulation models that isolate the ENSO signal have demonstrated its upward propagation into the stratosphere. Here we review the literature in this field and show results from the most recent version of the Whole Atmosphere Community Climate Model to illustrate the propagation and the mechanisms whereby the signal manifests itself in the stratosphere. The ENSO signal propagates upward to about 40 km by means of large-scale Rossby waves. The propagation is strongly influenced by the zonal mean zonal winds. Most of the strong ENSO events tend to peak in the boreal winter and so the ENSO signal is observed mainly at high latitudes during the Northern Hemisphere winter where the winds are westerly and allow Rossby wave propagation. The ENSO signal is also identified at polar latitudes in the Northern Hemisphere winter in the form of warmer temperatures and weaker winds during a strong El Niño event. This signal shows a zonally homogeneous behavior from the intensification of the stratospheric meridional circulation (in which air rises in the tropics and moves toward the winter pole where it descends) forced by anomalous propagation and dissipation of Rossby waves at middle latitudes during strong ENSO events.

Key words: **stratosphere dynamics; ENSO variability; climatology**

Introduction

The El Niño–Southern Oscillation (ENSO) is a coupled phenomenon of the ocean and the atmosphere. Its warm phase, or El Niño, refers to the ocean component of the system and is characterized by an anomalous warming in the eastern tropical Pacific, usually in the northern winter. The term *Southern Oscillation* refers to the variation in sea level pressure between the eastern Pacific and the Indian Ocean. ENSO is known to be one of the main sources of variability in the tropical troposphere and it has been related to changes in the jet stream, the strong westerly wind current concentrated at middle latitudes in the upper troposphere[1,2]; to variations in the Monsoon system over Asia and Australia[3–5]; and to changes in cyclone frequency over Europe.[6]

In the last few decades, many authors have analyzed the effects of ENSO, both in the tropics and extratropics. Typically, these studies have characterized the ENSO phenomenon by a pressure index, computed as the pressure difference between the eastern part and the western part of the Pacific Ocean, or by using a sea surface temperature (SST) index obtained by averaging SST over a selected region in the tropical eastern Pacific. Most authors have found a response in the tropical

Address for correspondence: Dr. Natalia Calvo, National Center for Atmospheric Research, Atmospheric Chemistry Division, P.O. Box 3000 Boulder, CO 80307-3000. Voice: +303-497-1894. calvo@ucar.edu

Trends and Directions in Climate Research: Ann. N.Y. Acad. Sci. 1146: 16–31 (2008).
doi: 10.1196/annals.1446.008

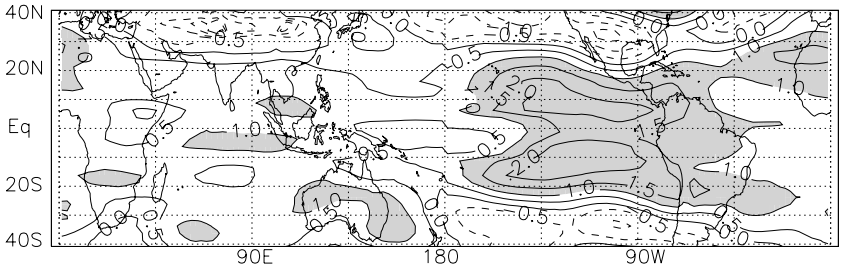

Figure 1. Microwave Sounding Unit (MSU T2lt) lower tropospheric temperatures for January 1998. The contour interval is 1 K. Negative contours are dashed. Shadowed regions indicate temperature anomalies higher than 1 K and show the characteristic horseshoe pattern.

troposphere that lags the ENSO index by 3–6 months, depending on the data set and index used.[3,7–11] The spatial distribution of the ENSO signal has also been widely analyzed. During its warm phase, or El Niño, the ENSO signal is characterized by an intense warming over the central and eastern Pacific as well as in most parts of the Indian Ocean and southeast of Africa.[10,12,13] In the tropical western Pacific the anomalies in temperature take the form of a "horseshoe pattern" with the two extremes pointing to the east. Observations of outgoing long-wave radiation (OLR; the energy emitted by the Earth as infrared radiation) and of the temperatures measured by the satellite-borne Microwave Sounding Unit (MSU) radiometers show that maximum warming occurs to the east of the precipitation anomalies that are observed around the dateline.[14] Figure 1 shows the anomalous pattern in the tropical lower troposphere for MSU temperatures in January 1998 during one of the strongest El Niño of the last century. The horseshoe pattern is highlighted in this figure in gray where the temperature anomalies are higher than 1 K.

The impacts of ENSO on temperature are also noticeable at middle latitudes, although the thermal response of the troposphere in these regions is not as intense as in the tropics. During a warm El Niño episode, an anomalous warming is observed in the northwest part of North America and the western part of South America, while an anomalous cooling is registered in the southeast of North America and the central part of the Andes. These anomalies that occur far away from the tropics are known as "teleconnections."

Theoretical and model studies have shown that the teleconnections are observed because convective activity in the tropical region generates Rossby waves (large-scale disturbances from the variation of the Coriolis force with latitude; see, e.g., Ref. 15), and, thus, anomalies in the distribution of convective activity generate changes in the atmospheric wave pattern[1,16] that in turn produce anomalies in temperature. Horel and Wallace[1] showed that the ENSO teleconnections in the Northern Hemisphere are observed only when the winds are westerly at low latitudes (in the winter half of the year when the Atlantic and Pacific troughs are displaced equatorward). The Pacific North America Pattern (PNA) is among the most important teleconnections related to ENSO in the Northern Hemisphere,[1,16] which in its positive phase produces above-average geopotential heights in the vicinity of Hawaii and over the intermountain region of North America and below-average geopotential height south of the Aleutian Islands and over the southeastern United States. Its relationship with ENSO is discussed in numerous papers.[1,17–19] In the Southern Hemisphere, the studies show anomalies related to ENSO in high-latitude regions, such as Antarctica, and in lower latitudes in Australia and South America.[19–23] In addition, ENSO also has an influence on two modes of variability in the Southern Hemisphere: the

Pacific South American pattern (PSA) and the Antarctic Oscillation (AAO).[24–27] Some studies have also shown that the response of atmospheric temperature to ENSO has a nonlinear component, that is, the response is not symmetrical for the warm (El Niño) and cold (La Niña) phases of the phenomenon.[28,29]

The behavior of ENSO appears to have been affected by the interdecadal change detected in several climatic variables that occurred at the end of the 1970s. On one hand, this change modified the development and evolution of the SST in the tropical Pacific.[29–32] After 1976/1977, the surface temperature warming developed in the western and central Pacific, extending later toward the eastern part of the basin,[10] while before that date the positive temperature anomalies were first observed along the west coast of South America and moved westward afterward, as shown in Rasmusson and Carpenter's[4] analysis of the 1951–1972 period. Furthermore, changes in the large-scale circulation patterns, such as an intensification of the PNA pattern during strong ENSO events, have occurred after 1979.[33,34] The origin of these changes is not well understood, although some works point to a major influence of the annual cycle during the ENSO events after the 1970s,[34] while others suggest a modulation of the tropical teleconnections from the Pacific Decadal Oscillation related to the SSTs in the North Pacific.[35]

The temporal evolution of the ENSO signal has also been widely studied. Kelly and Jones[36] identified two patterns of variability in the SST related to ENSO, with a lag of 3 months between them. In tropospheric temperature, Yulaeva and Wallace[14] also identified two different patterns lagged by 5 months. More recently, Calvo *et al.*[11] obtained three different spatial patterns in tropospheric temperatures related to ENSO and studied their temporal evolution. ENSO-related temperature anomalies occur initially as two different wave patterns; the first one precedes the full development of tropical SST anomalies and the second one develops simultaneously with it. These patterns appear to represent the equatorial wave response to anomalous latent heat release.[11,14] The zonally symmetric atmospheric warming that lags the development of the SST anomalies is interpreted as a diabatic response to changes in the surface energy balance during ENSO.[10,14]

Besides the ENSO signal in the troposphere, several recent studies have presented evidence that ENSO propagates upward and also has an effect in the stratosphere. This layer, where the temperature increases with height mainly from the absorption of ultraviolet radiation by ozone, spans the range of altitude from about 15 km in the tropics, or 8–10 km in the extratropics, to about 50 km. It thus lies between the troposphere (below) and the mesosphere (above). In this paper, we present an overview of the ENSO signal in the middle atmosphere, together with results from a new general circulation model that illustrate the propagation of the ENSO signal and the mechanisms by which the signal reaches the stratosphere. Section 2 reviews the literature on the stratospheric ENSO signal; Section 3 introduces the numerical model and methodology used in this paper; and Section 4 presents the main results. Conclusions are summarized in Section 5.

The ENSO Signal in the Stratosphere

The first works that studied the influence of ENSO in the stratosphere, by means of observations, were those of Wallace and Chang, van Loon and Labitzke, Hamilton, Baldwin and O'Sullivan, and Kodera *et al.*[37–41] However, the results of these studies are not uniformly consistent. Some of the studies show a relationship between ENSO and the large-scale cyclonic circulation observed over the polar region in the Northern Hemisphere stratosphere, usually known as the polar vortex. During a strong El Niño event, some authors found a weaker polar vortex together with an intensification of the high-pressure center located over the Aleutian region. Other authors do not find any statistically significant relationship between

ENSO and the stratosphere and they point out the difficulty of isolating the ENSO signal from other sources of variability that affect the Northern Hemisphere polar stratosphere in the short observational records available (between 20 and 30 years).

The effects of ENSO on temperature were studied in particular by Reid *et al.*,[42] who used several radiosonde stations in the Pacific Ocean, and Yulaeva and Wallace[14] and Calvo *et al.*,[11] who used MSU satellite temperatures over the tropical region. They all showed an ENSO signal in the tropical lower stratosphere of opposite sign to that in the troposphere. Some authors suggested that an intensification of the meridional circulation in the tropical troposphere, known as the Hadley cell, with air rising in the tropics and descending in the subtropics, might explain the opposite behavior in the troposphere and stratosphere.[42,43] However, Calvo *et al.*[11] explained the tropical stratospheric cooling over the eastern Pacific as the upper air manifestation of internal equatorial waves forced by anomalous convection in the troposphere from changes in SSTs. As we will show later, both explanations were reasonable as they refer to different behaviors of the ENSO manifestation in the atmosphere: its zonal-mean behavior and the wave-like ENSO signal, respectively.

Several problems have been found in the analysis of the ENSO signal in the stratosphere. First, ENSO is not one of the main sources of variability in this atmospheric layer as it is in the troposphere, and this makes it more difficult to identify its signal among those generated by other phenomena. Among the latter is the Quasi Biennial Oscillation (QBO), an oscillation of the stratospheric winds in the tropical region wherein the equatorial winds oscillate from westerlies to easterlies with a period of about 27 months. The QBO is known to shift the region where large-scale Rossby waves dissipate in the stratosphere either poleward or equatorward, depending on whether the winds in the tropics are easterly or westerly, and this can affect the interaction between the waves and the mean flow and, ultimately, the state of the stratosphere in the polar region.[38,44,45] The short records available make it difficult to stratify the observations according to QBO phases versus ENSO phases and, thus, to analyze both phenomena independently. Other additional sources of variability that might interfere with the detection of the ENSO signal in the stratosphere are volcanic eruptions, which inject aerosols into the lower stratosphere and can change the stratospheric composition and global circulation[46]; climate change related to the greenhouse gases, which affects the radiative balance near the tropopause and influences the local thermal structure and circulation[47]; and solar variability, which can generate chemical and dynamical changes in the stratosphere and mesosphere.[48,49]

An additional problem in analyzing the ENSO phenomenon in the stratosphere arises from the lack of global observations. The coarse horizontal resolution in observations and the few vertical levels typically available have made this analysis difficult. This is why in the last few years general circulation models (GCMs), with a global and homogeneous grid and the ability to isolate different sources of variability, have become one of the more important tools available to investigate the ENSO phenomenon in the middle atmosphere (the part of the atmosphere that includes the stratosphere and spans up to about 100 km).

Some of the early modeling studies simply compared model integrations with and without imposed SST anomalies in the tropical Pacific. They used models that included only a few levels in the lower stratosphere.[49–55] Eventually, other works dealt with the influence of SST variability on the polar stratosphere in the Northern Hemisphere, using simplified simulations with more complete models that included a more ambitious treatment of the middle atmosphere. Hamilton[56] reproduced ENSO variability in the stratosphere with the SKYHI model from the Geophysical Fluid Dynamics Laboratory in Princeton, New Jersey, using idealized SST perturbations typical of ENSO

events during winter months. The results were in very good agreement with the observational works discussed before and showed that ENSO events are associated with stationary large-scale Rossby wave perturbations of zonal wave numbers 1 and 2. One manifestation of these wave anomalies is the intensification of the Aleutian High in the middle stratosphere. Lahoz[57] studied the possible influence of the SST variability on the trends in temperature using a tropospheric–stratospheric version of the UK Meteorological Office Unified Model. An ensemble of nine simulations for winter conditions in the Northern Hemisphere from the 1980s to the 1990s showed that the UK Met Office Unified Model reproduced at least part of the observed temperature trend (cooling in the Northern Hemisphere lower stratosphere) with SST variations but did not find conclusive results in terms of the response to ENSO.

In the last few years, several multidecadal integrations have been run with GCMs. Usually several realizations of each model are obtained and the average of those realizations is computed to produce an ensemble average, or ensemble mean. Braesicke and Pyle[58] used the UK Met Office Unified Model to compare different ensembles with and without SST variability and obtained a weaker polar vortex with SST variability that does not appear to be related to extreme ENSO events. Some other works specifically focusing on ENSO effects are those of Sassi *et al.*,[59] with the Whole Atmosphere Community Climate Model, version 1 (WACCM1), developed at the National Center for Atmospheric Research (NCAR); Manzini *et al.*,[60] using the Middle Atmosphere European Center Hamburg Model MAECHAM5; and Garcia-Herrera *et al.*,[61] who compared in detail results from these two models and the European Center for Medium-range Weather Forecasts (ECMWF) reanalysis of atmospheric observations, ERA-40. None of the models used in these studies produced a QBO. Although this is a shortcoming of the models, it does have the advantage that it allows analysis of model results without this additional source of variability. These studies did find changes in the stratospheric circulation related to ENSO and showed the wave-like ENSO signal in the stratosphere and the way it propagates upward from the troposphere. In addition, they also revealed a new aspect not documented before: ENSO has an effect on stratospheric zonal mean temperature related to changes in the stratospheric mean meridional circulation.

Sassi *et al.*[59] showed anomalies that have the structure of planetary Rossby waves propagating up to the mesosphere and studied the momentum deposition by resolved and parameterized waves during strong ENSO events in the Northern Hemisphere. Manzini *et al.*[60] obtained a significant response in the zonal mean flow that had not been shown previously, with a weaker polar vortex during warm ENSO events but no significant signal from cold events (La Niña). In addition, an enhancement of the downward propagation of wave–mean-flow interaction in the middle atmosphere clearly appears in this model. The work of Garcia-Herrera *et al.*[61] shows good agreement between models and reanalysis, which highlights the robustness of the results. While most previous works focused on the Northern Hemisphere, this work also analyzes the ENSO signal in the tropical and Southern Hemisphere stratosphere comparing different latitudes. The direct influence of ENSO on the stratospheric circulation through changes in the upward propagation of Rossby waves and the relationship between these two is explicitly shown in this paper for the first time by means of wave activity and circulation velocities anomalies.

Model and Methodology

The WACCM3 is a GCM with interactive chemistry based on the US National Center for Atmospheric Research's Community Atmosphere Model (CAM3). It includes most of the physical and chemical processes that are important for describing the dynamics and chemistry of the atmosphere above the troposphere

and up to about 140 km. It has 66 vertical levels from surface up to about 140 km, and its vertical coordinate is isobaric above 100 hPa (approximately 16 km) but hybrid below that level. The vertical resolution is variable, ranging from 1.1 km in the troposphere, above the planetary boundary layer, to about 3.5 km in the upper atmosphere.

The model is used to simulate the period 1950–2004. As boundary conditions, SSTs are prescribed from the global Met Office Hadley Center, Exeter, U.K., data set prior to 1981 and from the Smith/Reynolds data set after 1981.[62] There is no QBO in the model, either internally generated or externally prescribed. As noted previously, this may be considered an advantage for our purposes as it allows study of the ENSO signal in isolation from this other important source of stratospheric variability. Chemical effects of volcanic aerosols are included but not their radiative effects. The 11-year solar cycle irradiance variability is parameterized in terms of the observed f10.7 radio flux. Detailed information about the model, processes, and parameterizations can be found in both Garcia *et al.*[63] and Richter *et al.*[64]

The main differences between WACCM3 and WACCM1 (which has also been used to study ENSO effects in the stratosphere, as noted above) include the use of Lin's finite volume formulation[65] for advection in WACCM3 as opposed to the semi-Lagrangian method used in WACCM1. The finite volume method is a mass-conserving approach to the solution of the governing equations in the model and is especially appropriate for modeling the advection of chemical species. In addition, WACCM3 includes interactive chemistry and solar cycle variability that were not incorporated in WACCM1.

The results presented here are based upon three realizations of WACCM3 run at horizontal resolution of $4^\circ \times 5^\circ$ (latitude × longitude). The ensemble average of the three realizations was computed for the period 1979–2000 in order to better compare with previous results that used the same period of analysis. Composites for the strongest El Niño and La Niña events were constructed and then the differences (El Niño minus La Niña averages) were analyzed.

TABLE 1. Central Month and Its Corresponding N3.4 Value for the Warmest and Coldest ENSO Events Considered in the Study

Warm ENSO Events		Cold ENSO Events	
January 1983	2.74	December 1984	−1.21
January 1992	1.82	November 1988	−1.91
December 1994	1.32	December 1998	−1.51
November 1997	2.76		

As noted in the Introduction, different indices can be used to characterize the ENSO phenomenon. We have chosen the Niño3.4 index (N3.4), which is the SST averaged over the region between long 120°W and 170°W and lat 5°S to 5°N. Warm and cold ENSO events have been chosen whenever this index exceeds 1.2 standard deviations (Table 1), as in Garcia-Herrera *et al.*[61] All the ENSO events peak in late fall–early winter except the strong warm ENSO event in August 1988, which has not been considered in this study to avoid misleading interpretation of the mechanisms involved since the stratospheric dynamics is strongly modulated by the seasonal cycle. In the composite analysis, month 0 indicates the month in which all the ENSO events reach their maximum N3.4 index value.

The significance of the anomalies with respect to internal natural variability has been computed by a Monte Carlo test following the methodology of Garcia-Herrera *et al.*[61] In the figures, the shadowed areas denote anomalies significant at the 95% confidence level.

Results

Wave-like ENSO Signal

Figure 2 displays the composite difference (El Niño minus La Niña) for monthly mean temperature anomalies at lat 40°N from month 0 to month 5. Shadowed regions denote the

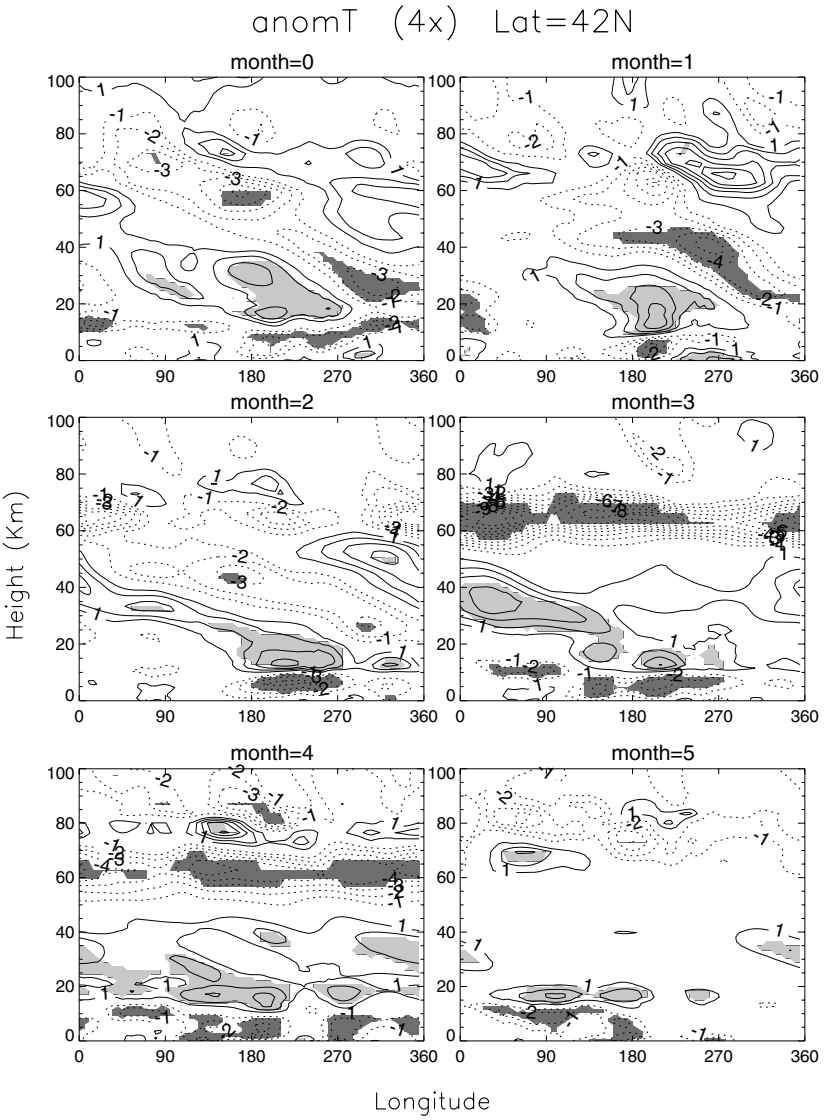

Figure 2. Composite differences (El Niño minus La Niña) of the temperature anomalies at lat 40°N from the WACCM3 ensemble simulation for months 0 to 5 after an El Niño event. Solid (dashed lines) denote positive (negative) anomalies. Light (dark) shadowed regions indicate positive (negative) statistically significant anomalies at the 95% confidence level. Contours are drawn every 1 K (zero line has not been displayed).

significant anomalies according to the Monte Carlo test mentioned in Section 3. The temperature anomalies show the upward propagation of the ENSO signal from the Pacific Ocean toward the middle atmosphere by means of large-scale Rossby waves, with negative anomalies in the troposphere and positive anomalies above the tropopause that tilt westward with height, indicating upward propagation. Rossby waves are generated in the troposphere mainly by large-scale orography, large-scale convective heating, and land–sea contrasts. From there, they propagate into the stratosphere primarily during winter because vertical propagation requires that the zonal wind be westerly (from west to east) and lower than a certain critical

value. This threshold depends on the spatial scale of the waves such that only ultralong Rossby waves (zonal wave numbers 1 to 3) are able to propagate into the stratosphere. These conditions are known as the Charney–Drazin criterion.[66] Significant anomalies are observed in WACCM3 during the first 5 months after the maximum of N3.4 index up to about 40 km altitude, in very good agreement with the results from the WACCM1 and MAECHAM5 models shown in Garcia-Herrera *et al.*[61] but with slightly smaller anomalies reaching higher altitudes than for the ERA-40 observational data set (see Figure 2 in Garcia-Herrera *et al.*[61]).

In the middle latitudes of the Southern Hemisphere, the ENSO propagation is not as effective as in the Northern Hemisphere (figure not shown), mainly because of the timing of the ENSO maxima with respect to the seasonal cycle. ENSO events tend to occur in the boreal winter, when stratospheric winds are westerly in the Northern Hemisphere and allow the vertical propagation of Rossby waves, in accordance with the Charney–Drazin criterion. However, in the Southern Hemisphere the winds are easterly in the boreal winter and this prevents upward wave propagation. Significant anomalies are observed in this case only in the troposphere and lower stratosphere below 20 km.

At tropical latitudes, a wave-like ENSO signal confined to the troposphere and lower stratosphere that shows composite differences (El Niño minus La Niña) for monthly mean temperature anomalies at lat 2°N is clearly observed in Figure 3. The wave-like ENSO signal has opposite signs in the troposphere and lower stratosphere as previous works have shown.[11,14] This is from the small vertical group velocities of tropical Rossby waves and the easterly winds that inhibit the propagation in this region. Beyond the lower stratosphere, the signal acquires a zonal symmetric behavior with the largest negative significant anomalies in month 3, which is known to be related to the mean meridional circulation as will be explained next.

Zonal Mean ENSO Signal

In addition to the wave-like signal, ENSO also generates anomalies in zonal mean fields. Figure 4 shows the composite differences (El Niño minus La Niña) for zonal mean temperature. WACCM3 shows a significant warmer polar stratosphere during a strong El Niño event, in good agreement with previous works (e.g., Refs. 59–61), up to 3 months after the maximum of the N3.4 index, accompanied by an anomalous cooling in the tropical stratosphere. The combination of warm and cold anomalies forms a dipole structure that propagates downward as time progresses, in good agreement with results shown in MAECHAM5 by Manzini *et al.*[60] The largest significant anomalies in WACCM3, both in the tropical and polar regions, are observed in month 3, with values up to 7 K at high latitudes. In the tropical region, the anomalous warming observed in the troposphere corresponds to the zonally symmetric anomalies that are observed to develop during the mature phase of a warm ENSO event.[11,14] Weaker zonal mean zonal winds are also observed (figure not shown) at high latitudes in the winter hemisphere during strong El Niño events accompanied by the warm anomalies, as expected from geostrophic balance.

Wave–Mean-flow Interaction

The generally accepted mechanism that explains the ENSO signal in the polar winter stratosphere involves the propagation and dissipation of Rossby waves at middle latitudes and their interaction with the zonal mean flow. In order to analyze in depth this mechanism, we have studied the propagation and dissipation of the Rossby waves in the stratosphere in WACCM3 and their impact on the stratospheric branch of the mean meridional circulation, also known as the Brewer Dobson circulation, which moves air from the tropical lower stratosphere to the polar regions in the winter hemisphere. These anomalies in the meridional

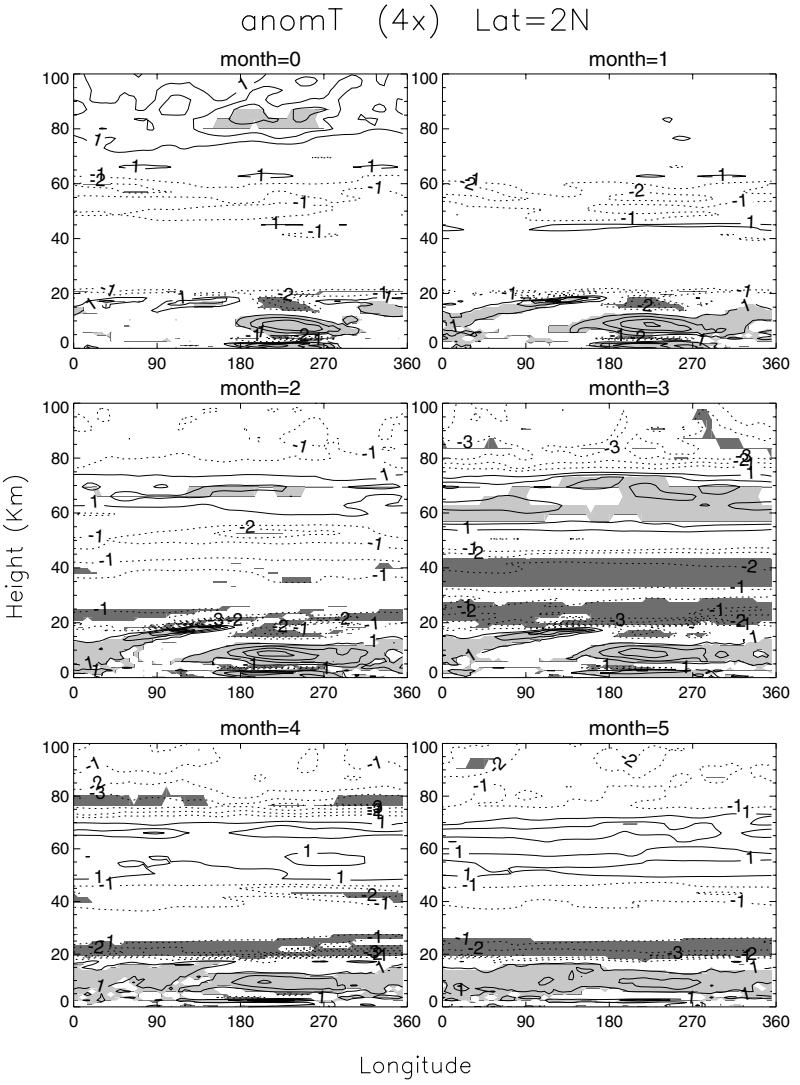

Figure 3. As Figure 1 at lat 2°N.

circulation are known to generate the anomalies in the zonal mean zonal wind and temperature in the polar region as we will explain next.

The propagation of the Rossby waves can be visualized using the Eliassen Palm flux (EP flux), which can be considered as a measure of the propagation of wave activity.[67] The divergence of the EP flux is a direct measure of the forcing of the mean flow by the wave perturbations[15,67] so that negative values of the EP flux divergence indicate regions where Rossby waves are dissipating and transfer momentum to the zonal mean flow. Figure 5 shows the composite difference (El Niño minus La Niña) of the EP flux anomalies (arrows) and its divergence anomalies (contours) from month 0 to month 5. The upward Rossby wave propagation is intensified (upward anomalies) from month 1 to month 5 in the Northern Hemisphere. As expected, the winter climatology [December, January, February (DJF)] in WACCM3 (Fig. 6) for the period 1979–2000 shows westerly winds in the Northern Hemisphere and easterly winds in the Southern Hemisphere during the boreal winter. Thus, following the Charney–Drazin

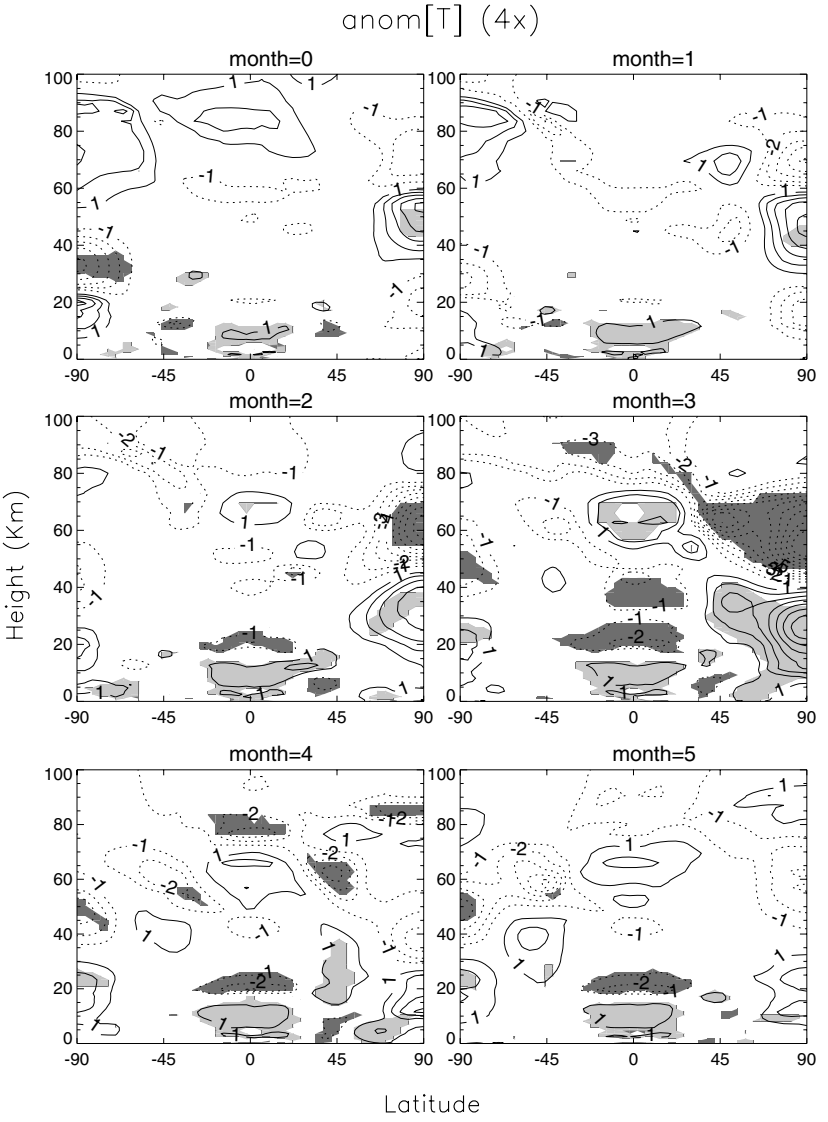

Figure 4. As Figure 1 for zonal mean temperature anomalies.

criterion explained above, westerly winds favor the upward wave propagation observed in Figure 5 during strong ENSO events in the Northern Hemisphere. Together with the increased EP flux, negative EP flux divergence is observed at middle latitudes in the stratosphere with the largest values during months 2 and 3 indicating strong wave dissipation in those regions.

These anomalies in the EP flux divergence are accompanied by an intensification of the mean meridional circulation. Figure 7 displays the composite difference of the anomalies of the mean meridional circulation (V*, W*) together with the anomalies in the EP flux divergence also shown in Figure 5. From month 1 to month 5, a clear intensification of the stratospheric circulation is observed, corresponding to the anomalous wave dissipation indicated by the EP flux divergence anomalies. This accelerated circulation moves air from the lower tropical stratosphere to the polar stratosphere in the Northern Hemisphere. The rising air in the tropics generates adiabatic cooling as observed

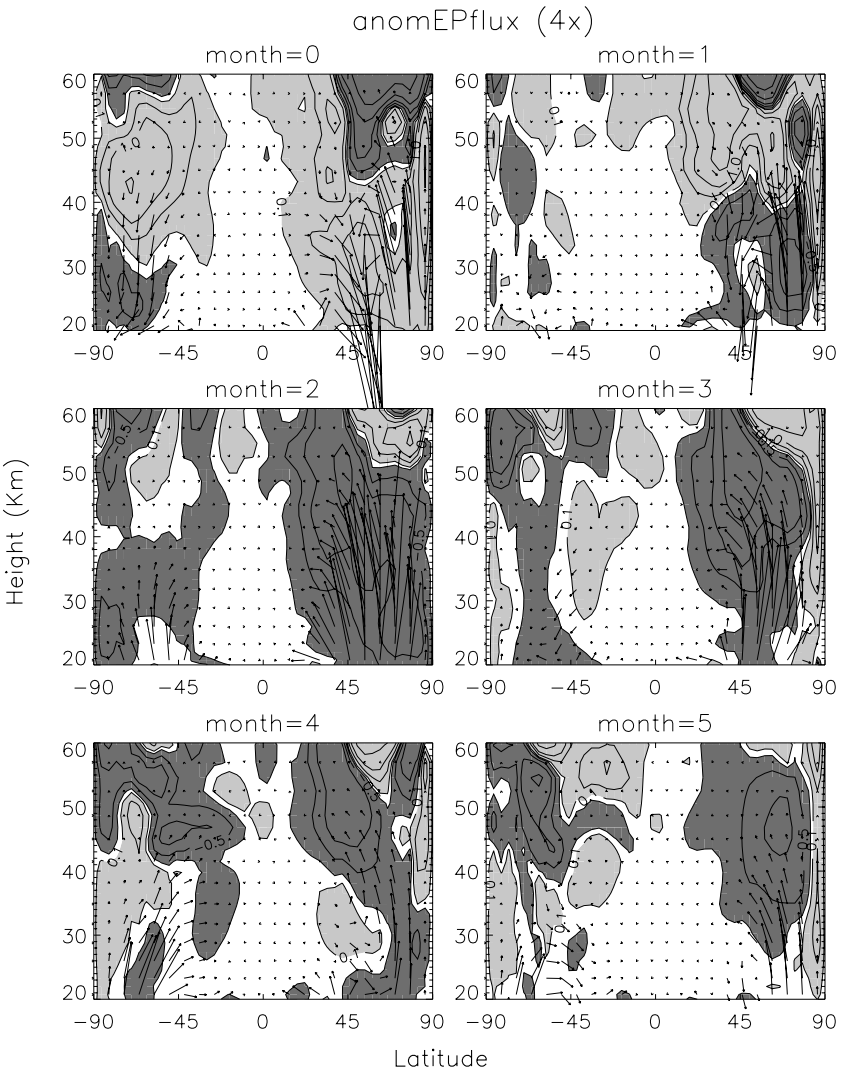

Figure 5. Composite differences (El Niño minus La Niña) for the EP flux anomalies (arrows) and its divergence (contours) anomalies for months 0 to 5 after an El Niño event. EP flux values drawn are Fy $\times$ 10^{-5} kg s^{-2} and Fz $\times$ 10^{-3} kg s^{-2}. Contours of the EP flux divergence are drawn at $\pm$0.1, 0.5, 1, 2, 4 m s^{-1} day^{-1}. Shadow regions for EP flux divergence anomalies larger than $\pm$0.1 m s^{-1} day^{-1}: light (dark) shadowed for positive (negative) values.

there (see Fig. 4), while the descending air in the polar region produces the polar adiabatic warming.

In short, WACCM3 results show that, during the warm phase of ENSO, a more intense Rossby wave propagation and dissipation occurs at middle and high latitudes in the Northern Hemisphere. As they dissipate, the planetary waves deposit easterly momentum, which decelerates the mean westerly flow in the Northern Hemisphere stratosphere. The wave dissipation also alters the extratropical angular momentum balance and forces a stronger mean meridional circulation that in turn gives rise to tropical cooling and high-latitude warming at high latitudes, as has been shown in Figure 5. Figure 8 summarizes all the processes and interactions described above.

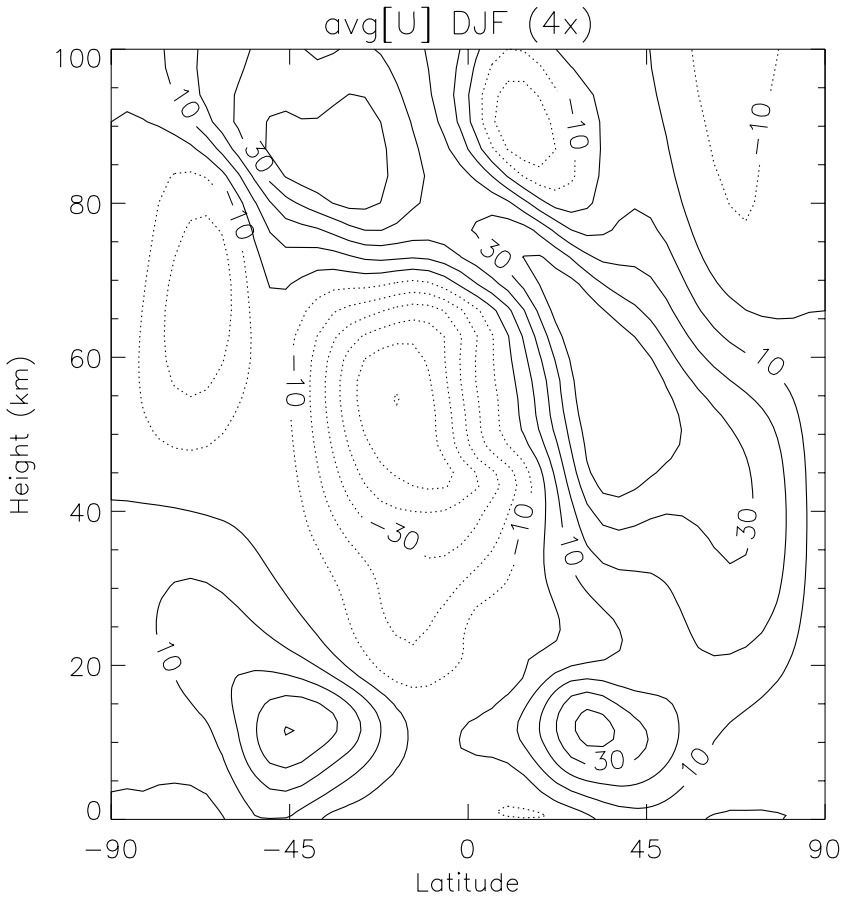

Figure 6. Winter climatology (December, January, February) of the zonal mean zonal winds for the period 1979–2000. Contours are drawn every 10 m s^{-1}; solid (dashed) contours for westerly (easterly) winds.

Summary

This paper has reviewed the literature on ENSO effects in the stratosphere. The main difficulties traditionally found in the study of the ENSO signal in the stratosphere have been discussed here; namely the lack of global observations and the fact that ENSO is not always the major source of variability in the stratosphere, which makes it difficult to disentangle its signal from other sources of variability. For these reasons, GCMs able to isolate the ENSO signal have become widely used in the study of the ENSO effects in the stratosphere. Results from the most recent version of the Whole Atmosphere Community Climate Model (WACCM3) have been presented here to illustrate the current theoretical understanding of the propagation of ENSO effects from the troposphere into the stratosphere. The ENSO signal propagates from the troposphere to the stratosphere, up to about 40 km height, in the form of Rossby waves. This is mainly observed at middle latitudes in the Northern Hemisphere during winter months because ENSO tends to peak in the northern winter when stratospheric winds are westerly in the Northern Hemisphere and allow vertical propagation of Rossby waves. In addition, the dissipation of Rossby waves at middle latitudes, which deposits easterly momentum on the background flow, weakens the polar vortex and intensifies the stratospheric

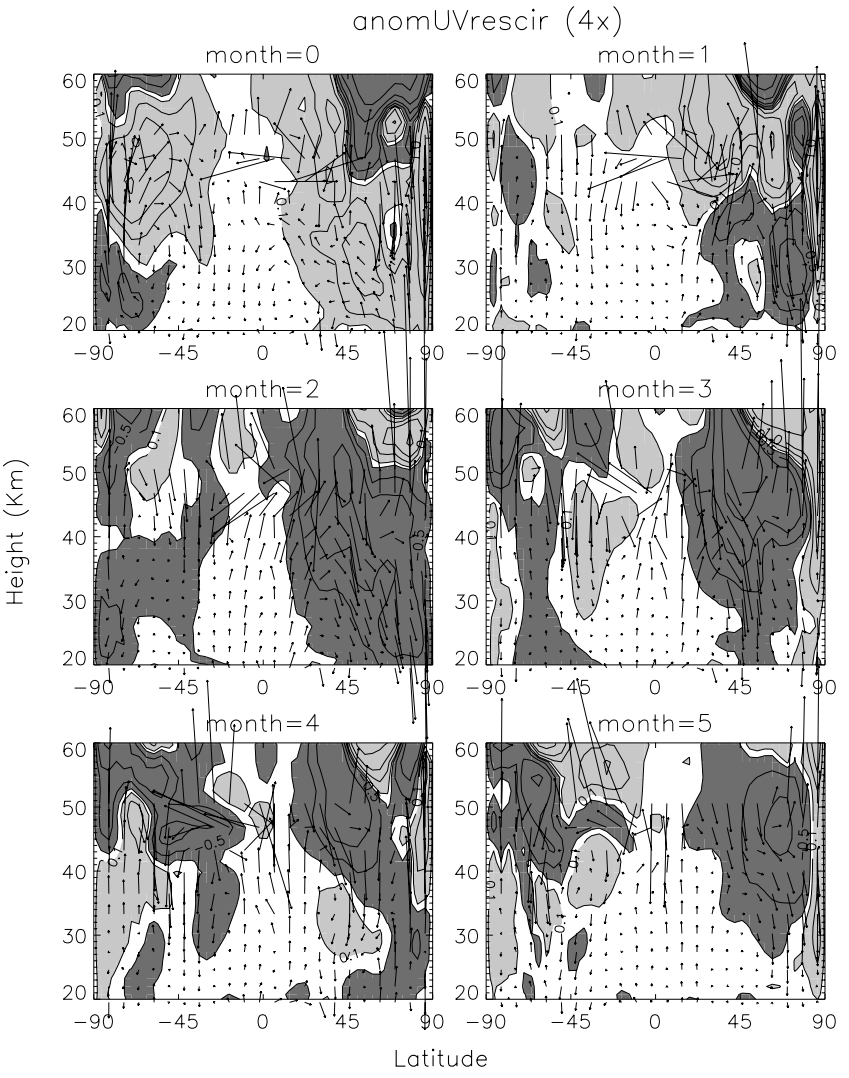

Figure 7. As Figure 4 for the meridional mean circulation velocities anomalies (arrows) and the EP flux divergence (contours) anomalies. Values of the meridional circulation are shown in 0.1 m s^{-1}. Contours of the EP flux divergence are drawn at ±0.1, 0.5, 1, 2, 4 m s^{-1} day^{-1}. Shadow regions are for EP flux divergence anomalies larger than ±0.1 m s^{-1} day^{-1}.

mean meridional circulation. This circulation, which moves air from the tropical lower stratosphere to the winter polar regions with air rising in the tropics and descending at high latitudes, gives rise to an anomalous polar warming (and tropical cooling) a few months after the maximum of the N3.4 index in the Northern Hemisphere.

There are still some aspects of the stratospheric ENSO signal that remain uncertain, since the results from the different data sets analyzed in different studies do not agree completely as regards the timing, location, and magnitude of the significant anomalies. Because differences among model simulations can arise from the internal variability of each model, additional experiments with different GCMs are required to increase the significance and robustness of the results and it is hoped to reduce the disparities among the models. Further

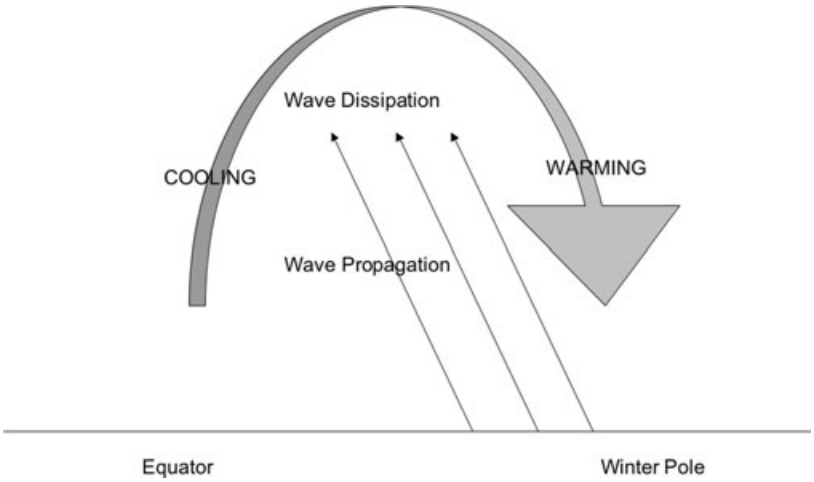

Figure 8. Main mechanisms involved in the propagation of the ENSO signal in the stratosphere. The thin arrows indicate the anomalous wave propagation and point to the wave dissipation region. The gray arrow indicates the air movement by the intensification of the stratospheric mean meridional circulation from anomalous wave dissipation. As a result, the air cools down in the tropical stratosphere and warms up at polar latitudes in the Northern Hemisphere as is indicated in the figure.

improvements in middle atmospheric modeling and also a better understanding of the relationships involved in wave–mean-flow interaction are still required to assess the remaining uncertainties.

Acknowledgments

This work has been funded by the Spanish Ministry of Education and Science and the Fulbright Commission in Spain. The WACCM3 simulations discussed here were carried out at the Barcelona Supercomputing Center, Barcelona, Spain, and at the National Center for Atmospheric Research (NCAR), Boulder, CO, USA. NCAR is sponsored by the US National Science Foundation.

Conflicts of Interest

The authors declare no conflicts of interest.

References

1. Horel, J.D. & J.M. Wallace. 1981. Planetary-scale atmospheric phenomena associated with the Southern Oscillation. *Mon. Wea. Rev.* **109:** 813–829.
2. Wang, H. & R. Fu. 2000. Influences of ENSO SST anomalies and winter storm tracks on the interannual variability of upper-troposphere water vapor over the Northern Hemisphere extratropics. *J. Clim.* **13. N.1:** 59–73.
3. Angell, J.K. 1981. Comparison of variations in atmospheric quantities with sea surface temperature variations in the equatorial eastern Pacific. *Mon. Wea. Rev.* **109:** 230–243.
4. Rasmusson, E.M. & T.H. Carpenter. 1982. Variations in tropical sea surface temperature and surface wind fields associated with the Southern Oscillation/El Niño. *Mon. Wea. Rev.* **110:** 354–384.
5. Lau, K.M. & H.T. Wu. 2000. Intrinsic coupled ocean-atmosphere modes of the Asian summer monsoon: a re-assessment of monsoon-ENSO relationships. *J. Clim.* **14:** 2880–2895.
6. Fraedrich, K. 1990. European grosswetter during the warm and cold extremes of the El Niño/Southern Oscillation. *Int. J. Climatol.* **10:** 12–31.
7. Angell, J.K. 2000. Tropospheric temperature variations adjusted for El Niño, 1958–1998. *J. Geophys. Res.* **105:** 11841–11849.
8. Jones, P.D. 1989. The influences of ENSO on global temperatures. *Clim. Monit.* **17:** 80–89.
9. Christy, J.R. & R.T. McNider. 1994. Satellite greenhouse signal. *Nature* **367:** 325.
10. Trenberth, K.E. *et al.* 2002. Evolution of El Niño-Southern Oscillation and global atmospheric surface temperatures. *J. Geophys. Res.* **107:** doi:10.1029/2000JD000298.

11. Calvo, N. *et al.* 2004. Analysis of the ENSO signal in tropospheric and stratospheric temperatures observed by MSU, 1979–2000. *J. Clim.* **17:** 3934–3946.
12. Kiladis, G.N. & H.F. Diaz. 1989. Global climatic anomalies associated with extremes in the Southern Oscillation. *J. Clim.* **2:** 1069–1090.
13. Trenberth, K.E. & J.M. Caron. 2000. The Southern Oscillation revisited: sea level pressures, surface temperatures and precipitation. *J. Clim.* **13:** 4358–4365.
14. Yulaeva, E. & J.M. Wallace. 1994. The signature of ENSO in global temperature and precipitation fields derived from the Microwave Sounding Unit. *J. Clim.* **7:** 1719–1736.
15. Andrews, D.G. *et al.* 1987. Middle Atmosphere Dynamics. *International Geophysics Series.* Volume 40. 489 pp. Academic Press Inc. New York.
16. Wallace, J.M. & D. S. Gutzler. 1981. Teleconnections in the Geopotencial Height Field during the Northern Hemisphere Winter. *Mon. Wea. Rev.* **109:** 784–812.
17. Hoskins, B.J. & D. Karoly. 1981. The steady linear response of a spherical atmosphere to thermal and orographic forcing. *J. Atmos. Sci.* **38:** 1179–1196.
18. Simmons, A.J. *et al.* 1983. Barotropic Wave Propagation and Instability, and Atmospheric Teleconnection Patterns. *J. Atmos. Sci.* **40:** 1363–1392.
19. Ribera, P. & M. Mann. 2002. Interannual variability in the NCEP reanalysis 1948–1999. *Geophys. Res. Lett.* **29:** doi:10.1029/2001GL013905.
20. van Loon, H. & R.A. Madden. 1981. The Southern Oscillation. Part I: Global Associations with Pressure and Temperature in Northern Winter. *Mon. Wea. Rev.* **109:** 1150–1162.
21. Ropelewski, C.F. & M.S. Halpert. 1987. Global and regional scale precipitation patterns associated with the el Niño/Southern Oscillation. *Mon. Wea. Rev.* **115:** 1606–1626.
22. Aceituno, P. 1988. On the Functioning of the Southern Oscillation in the South American Sector. Part I: Surface Climate. *Mon. Wea. Rev.* **116:** 505–524.
23. Robertson, A.W. & C.R.Mechoso. 1998. Interannual and Decadal Cycles in River Flows of Southeastern South America. *J. Clim.* **11:** 2570–2581.
24. Venegas, S. A. *et al.* 2001. Coupled oscillations in Antarctic sea-ice and atmosphere in the South Pacific sector. *Geophys. Res. Lett.* **28:** 3301–3304.
25. Karoly, D.J. 1989. Southern Hemisphere Circulation Features Associated with El Niño-Southern Oscillation Events. *J. Clim.* **2:** 1239–1252.
26. Garreaud, R.D. & D.S. Battisti. 1999. Interannual (ENSO) and Interdecadal (ENSO-like) Variability in the Southern Hemisphere Tropospheric Circulation. *J. Clim.* **12:** 2113–2123.
27. Carril, A.F. & A. Navarra. 2001. Low-frequency variability of the Antarctic Circumpolar wave. *Geophy. Res. Lett.* **28:** 4623–4626.
28. Yarnal, B. & H. Diaz. 1986. Relationships between extremes of the Southern Oscillation and the winter climate of the Anglo-American Pacific Coast. *Int. J. Clim.* **6:** 191–219.
29. Hoerling, M.P. *et al.* 1997. El Niño, La Niña, and the Nonlinearity of Their Teleconnections. *J. Clim.* **10:** 1769–1786.
30. Wang, B. 1995. Interdecadal changes in El Niño onset in the last four decades. *J. Clim.* **8:** 267–286.
31. An, S.I. & B.Wang. 2000. Interdecadal Change of the Structure of the ENSO Mode and Its Impact on the ENSO Frequency. *J. Clim.* **13:** 2044–2055.
32. Trenberth, K.E. & D.P.Stepaniak. 2001. Indices of El Niño Evolution. *J. Clim.* **14:** 1697–1701
33. Graham, N.E. 1994. Decadal-scale climate variability in the tropical and North Pacific during the 1970s and 1980s: observation and model results. *Clim. Dyn.* **10:** 135–162.
34. Diaz, H.F. *et al.* 2001. ENSO variability, teleconnections and climate change. *Int. J. Clim.* **21:** 1845–1862.
35. Gershunov, A. & T.P. Barnett. 1998. Interdecadal Modulation of ENSO Teleconnections. *Bull. Amer. Meteorol. Soc.* **79:** 2715–2725.
36. Kelly, P.M. & P.D. Jones. 1996. Removal of El Niño-Southern Oscillation signal from the gridded surface air temperature data set. *J. Geophys. Res.* **101:** 19,013–19,022.
37. Wallace, J. M. & F.-C. Chang. 1982. Interannual variability of the wintertime polar vortex in the Northern Hemisphere middle stratosphere. *J. Meteor. Soc. Jpn.* **60:** 149–155.
38. van Loon, H. & K. Labitzke. 1987. The Southern Oscillation. Part V: The anomalies in the lower stratosphere of the Northern Hemisphere in winter and a comparison with the quasi-biennial oscillation. *Mon. Wea. Rev.* **109:** 149–155.
39. Hamilton, K. 1993. An examination of observed Southern Oscillation effects in the Northern Hemisphere stratosphere. *J. Atmos. Sci.* **50:** 3468–3473.
40. Baldwin, M.P. & D.J. O'Sullivan. 1995. Stratospheric effects of ENSO-related tropospheric circulation anomalies. *J. Clim.* **8:** 649–667.
41. Kodera, K. *et al.* 1996. Interannual variability of the winter stratosphere and troposphere in the Northen Hemisphere. *J. Meteor. Soc. Jpn.* **74:** 365–382.
42. Reid, G.C., K.S. Gage & J.R. McAfee. 1989. The thermal response of the tropical atmosphere to variations in equatorial Pacific sea surface temperature. *J. Geophys. Res.* **94:** 14705–14716.
43. Pan, Y.H. & A.H. Oort. 1983. Global climate variations connected with sea surface temperature anomalies in the eastern tropical Pacific Ocean for

the 1958–1973 period. *Mon. Wea. Rev.* **111:** 1244–1258.
44. Holton, J.R. & H.C. Tan. 1980. The Influence of the Equatorial Quasi-Biennial Oscillation on the Global Circulation at 50 mb. *J. Atmos. Sci.* **37:** 2200–2208.
45. Calvo, N., M.A. Giorgetta & C. Pena-Ortiz. 2007. Sensitivity of the boreal winter circulation in the middle atmosphere to the quasi-biennial oscillation in MAECHAM5 simulations. *J. Geophys. Res.* **112:** D10124, doi:10.1029/2006JD007844.
46. Granier, C. & G.P. Brasseur. 1992. Impact of heterogeneous chemistry on predictions of ozone changes. *J. Geophys. Res.* **97:** 18015–18033.
47. Austin, J., N. Butchart & K.P. Shine. 1992. Possibility of an Arctic ozone hole in a doubled-CO_2 climate. *Nature* **360:** 221–225.
48. Hood, L.L., J.L.Jirikowic & J.P. McCormack. 1993. Quasi-Decadal Variability of the Stratosphere: Influence of Long-Term Solar Ultraviolet Variations. *J. Atmos. Sci.* **50:** 3941–3958.
49. Labitzke, K. & H. van Loon. 1997. The signal of the 11-year sunspot cycle in the upper troposphere-lower stratosphere. *Spa. Sci. Rev.* **80:** 393–410.
50. Keshavamurty, R.N. 1982. Response of the atmosphere to sea surface temperature anomalies over the equatorial Pacific and the teleconnections of the Southern Oscillation. *J. Atm. Sci.* **39:** 1241–1259.
51. Blackmon, M.L., J.E. Geisler & E.J. Pitcher. 1983. A general circulation model study of the January climate anomaly pattern associated with interannual variation of equatorial Pacific sea surface temperatures. *J. Atm. Sci.* **40:** 1410–1425.
52. Shukla, J. & J.M.Wallace. 1983. Numerical simulation of the atmospheric response to equatorial Pacific sea surface temperature anomalies. *J. Atm. Sci.* **40:** 1613–1630.
53. Boer, J.G. 1985. Modeling the atmospheric response to the 1982/83 El Nino. In *Coupled Ocean-Atmosphere Models*, C.J.C. Nihoul, Ed.: 7–17. Elsevier. Amsterdam.
54. Lau, N.-C. 1985. Modelling the seasonal dependence of the atmospheric response to observed El Niños in 1962–76. *Mon. Wea. Rev.* **113:** 1970–1996.
55. Lau, N.-C. & M.J. Nath. 1990. A general circulation model study of the atmospheric response to extratropical SST anomalies observed in 1960–1979. *J. Clim.* **3:** 965–989.
56. Hamilton, K. 1993. A general circulation model simulation of El Niño effects in the extratropical Northern Hemisphere stratosphere. *Geophys. Res. Lett.* **20:** 1803–1806.
57. Lahoz, W.A. 2000. Northern Hemisphere winter stratospheric variability in the Met. Office Unified Model. *Quart. J. Roy. Meteorol. Soc.* **126:** 2605–2630.
58. Braesicke, P. & A. Pyle. 2004. Sensitivity of dynamics and ozone to different representations of SSTs in the Unified Model. *Quart. J. Roy. Meteorol. Soc.* **99:** 1–9.
59. Sassi, F. *et al.* 2004. The effects of ENSO on the Dynamical, thermal and Chemical Structure of the Middle Atmosphere. *J. Geophys. Res.* **109:** doi:10.1029/2003JD004434.
60. Manzini, E. *et al.* 2006. The influence of sea surface temperatures on the Northern winter stratosphere: Ensemble simulations with the MAECHAM5 model. *J. Clim.* **19:** 3863–3881.
61. Garcia-Herrera, R. *et al.* 2006. Propagation of ENSO temperature signals into the middle atmosphere: A comparison of two general circulation models and ERA-40 reanalysis data. *J. Geophys. Res.* **111:** D06101, doi:10.1029/2005JD006061.
62. Hurrel, J.W. *et al.* 2006. The dynamical simulation of the Community Atmospheric Model version 3 (CAM3). *J. Clim.* **19:** 2162–2183.
63. Garcia, R. *et al.* 2007. Simulation of secular trends in the middle atmosphere, 1950–2003. *J. Geophys. Res.* **112:** D09301, doi:10.1029/2006 JD007485.
64. Richter, J. *et al.* 2008. Dynamics of the middle atmosphere as simulated by the Whole Atmosphere Community Climate Model, version 3 (WACCM3). *J. Geophys. Res.* 113, D08101, doi:10.1029/2007JD009269.
65. Lin, S.J. 2004. A "vertically-Lagrangian" finite-volume dynamical core for global atmospheric models. *Mon. Wea. Rev.* **132:** 2293–2307.
66. Charney, J.G. & P.G. Drazin. 1961. Propagation of planetary-scale disturbances from the lower into the upper atmosphere. *J. Geophys. Res.* **66:** 83–109.
67. Edmon, H.J. Jr., B.J. Hoskins & M.E. McIntyre. 1980. Eliassen-Palm cross sections for the Troposphere. *J. Atmos. Sci.* **37:** 2600–2616.